



micro-Raman and micro-Photoluminescence study of ZnO thin films

M.A. Urbina-Yarupetan¹ and J.C. Gonzalez*^{2,3}

¹ Universidad Nacional Mayor de San Marcos, Facultad de Ciencias Físicas. Lima, Perú

² Universidad de Ingeniería y Tecnología (UTEC), Laboratorio de Física de Materiales e Ingeniería de Superficies. Lima, Perú

³ Instituto de Ciencia de Materiales de Sevilla – CSIC, Grupo de Investigación de Superficies, Intercaras y Láminas Delgadas. Sevilla, España

Recibido 21 setiembre 2020 – Aceptado 02 diciembre 2020

Abstract

We present the experimental results of optical analysis of nanostructured ZnO thin films grown onto commercial glass by reactive sputtering. Films with 20, 50, and 100 nm in thickness were analyzed by micro-Raman and micro-photoluminescence spectroscopies. Raman and photoluminescence bands were deconvoluted with Lorentzian profiles, in order to obtain information about response of films to excitation with laser light, occurring changes in position, full width half maximum (FWHM), and area of each phonon and emission bands of ZnO, correlating them with its nanostructure nature, and packing morphology of ZnO nanocolumns.

Keywords: Nanostructured thin films, micro-Raman spectroscopy, micro-Photoluminescence spectroscopy.

Estudio micro-Raman y micro-Fotoluminiscente de capas delgadas de ZnO

Resumen

Presentamos los resultados experimentales del análisis óptico de capas delgadas nanoestructuradas de ZnO crecidas sobre vidrio comercial por pulverización catódica reactiva. Las capas delgadas con 20, 50 y 100 nm de espesor fueron analizadas por espectroscopias micro-Raman y micro-fotoluminiscencia. Las bandas Raman y de fotoluminiscencia se desconvolucionaron con perfiles Lorentzianos, para obtener información sobre la respuesta de las capas a la excitación con luz láser, a través de los cambios en la posición, el anchura a media altura y el área de cada banda fonónica y de emisión del ZnO, correlacionándolo con su naturaleza nanoestructural, y la morfología de empaquetamiento de las nanocolumnas de ZnO.

Palabras clave: Capas delgadas nanoestructuradas, Espectroscopía micro-Raman, Espectroscopía micro-Fotoluminiscente.

Introduction

The ZnO semiconductor compound has unique and interesting properties, for that reason it has received considerable attention for its wide range of applications in the area of materials science [Wan08] [Ish06]. Also, ZnO has a multiplicity of morphologies [Pan01] at nanoscale, this is the reason of its versatile applications. Its wide band-gap (energy 3.37 eV) and fast electron transfer kinetics [Zho06] enables huge potential in electronic appli-

ances [Bha05] [Ko003]. Moreover, the polarity of ZnO surfaces allows a wide range of nanostructures such as rings, springs, and helices [Wan04]. The physical properties of semiconducting nanocrystallites are dominated by the spatial confinements of electronic and vibrational excitations [Veg14].

The nanocolumns in nanostructured ZnO thin film are a good niche to study its physical properties through of vibrational spectrum [Arg69]. Raman spectroscopy

*juanc.gonzalez@icmse.csic.es

is a technique typically used to determine the vibrational phononic modes through the interaction of laser light with matter while photoluminescence spectroscopy is other technique used to perform light emission from any form of matter after the absorption of photons. Both techniques were employed to study vibrational and optical spectrum of ZnO semiconducting thin films.

Experimental

ZnO thin films have been grown by the reactive magnetron sputtering technique onto commercial glass, experimental growth conditions are described in reference [Urb20].

micro-Raman Spectroscopy

The measurements of the spontaneous Raman and photoluminescence spectra were carried out using a RH800 Horiba-Jobin-Yvon Raman spectrometer (Figure 1a - b), equipped with a holographic network of 600 lines/mm and 2 cm^{-1} of spatial resolution, attached with Peltier air-cooled CCD detector. In addition, the spectrometer has attached an Olympus BX-41 confocal metallographic microscope. The Raman spectrometer was previously calibrated by using a silicon wafer ($\omega_{Si} = 521 \text{ cm}^{-1}$). YAG solid-state laser ($\lambda = 532 \text{ nm}$) in the visible, and He-Ne gas laser ($\lambda = 325 \text{ nm}$) in the ultraviolet were employed as excitation source, for the spontaneous Raman and photoluminescence spectra, respectively.

Spontaneous Raman spectra were recorded in backscatter geometry (Figure 1c), and the penetration depth (δ) of laser light was $\delta \sim 5.26 \text{ }\mu\text{m}$ [Pol08] for ZnO (bulk) at 532 nm. The laser power was kept as low as possible (0.5 mW) to avoid degradation of the sample, by using neutral filters, but enough to produce good quality spectra in a reasonable time, in order to obtain a compromise between data to noise. An optical objective of $\times 100$ magnification was used for measurements in the visible range (spot size $\sim 1 \text{ }\mu\text{m}$ in diameter), while 5 seconds of exposure time, and 20 seconds for accumulation was employed for spectra recording. The range of measurements was from 200 to 900 cm^{-1} . All measurements were carried out at room temperature and band shifts or shape changes of the spectra were never observed during acquisition. We determine the intensities of the ZnO Raman phononic bands by fitting them with a Lorentzian profile plus a constant background term. Lorentzian profile of these modes has been described in reference [Yua17]:

$$I_{Raman} = I_0 + \frac{2A}{\pi} \frac{\Gamma}{4(\omega - \omega_0)^2 + \Gamma^2} \quad (1)$$

where A is the area of the curve, ω_0 is the frequency of the phonon for this mode and Γ is the full width half maximum of the profile.

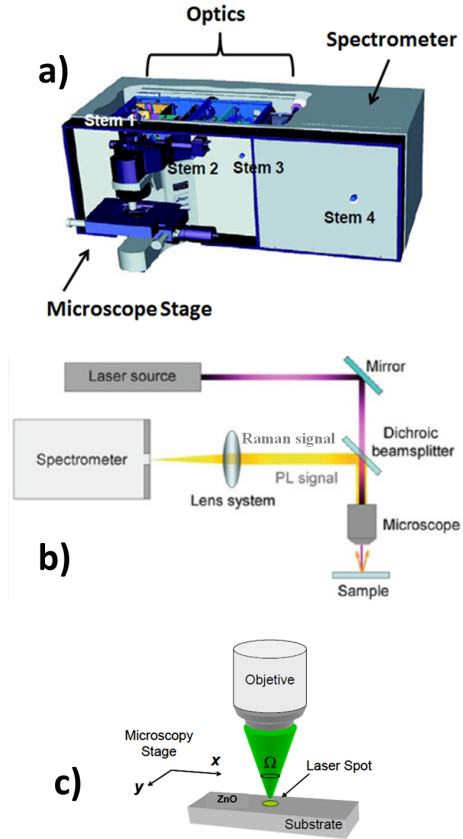


Figure 1: a) Draw of RH800 Horiba-Jobin-Yvon Raman spectrometer, b) Experimental set-up, and c) Solid angle Ω in the light collection configuration called backscattering.

micro-Photoluminescence Spectroscopy

Photoluminescence spectra were acquired using the same Raman spectrometer described in the previous paragraph, but by changing the scattered light detection configuration from cm^{-1} to nm. Also, He-Ne laser was used ($\lambda = 325 \text{ nm}$), and selecting a $\times 40$ optical objective with quartz lens (spot size $\sim 2.5 \text{ }\mu\text{m}$ in diameter). The penetration depth (δ) was $\delta \sim 177.7 \text{ nm}$ [Pol08] for ZnO (bulk) at 325 nm. Then, ZnO thin films were placed under the objective and illuminated by UV laser beam (figure 1b). The measurement range was from 370 to 1000 nm while 3 seconds of exposure time and 3 seconds for accumulation were required for recording the spectra. We did not approach to 325 nm in order to avoid damaging the CCD detector, and the ZnO photoluminescence bands were in the selected measurement range (370 to 1000 nm). A fluorescent emission spectrum was obtained, and then the emission intensity variation of the ZnO sample was measured in the range of 370 to 1000

nm. We determined the intensities of the emission bands through the spectra fit with Lorentzian profiles by using equation (1).

Results and Discussion

Figure 2 shows the representative spontaneous Raman spectra of the three ZnO samples studied. It can be seen that the Raman signal and the spectrum background improve as more ZnO is deposited onto glass substrate, due to increasing of interaction volume and high value of penetration depth (δ). Raman spectra of the three films have been taken with the same exposition and accumulation times, in order to do comparisons. Moreover, the Raman bands as well as X-ray diffraction profiles, are directly related to the amount of matter present in the interaction volume [Cul56]. Also, the width of the Raman band (Γ) is in clear relation to the crystallinity of the thin films under study.

Figure 3 displays the spectra fitted with Lorentzian profiles according to equation (1). It was not possible to observe the Raman mode at 101 cm^{-1} (see table 1) because the Raman spectrometer has a Notch filter that exponentially decreases the intensity of the Rayleigh signal in the range of 0 to 200 cm^{-1} ($\omega = 0 \text{ cm}^{-1}$ is the laser frequency); therefore, only spontaneous Raman signals have been analyzed in the range of 200 to 900 cm^{-1} . Table 2 shows the parameters obtained from the fit, such as center position of the band ω (cm^{-1}), profile width Γ (cm^{-1}) and area A. The value of the figure of merit (χ^2) for the three thin films of 20 , 50 and 100 nm in thick-

ness was 0.69881 , 0.88546 , and 0.91098 respectively.

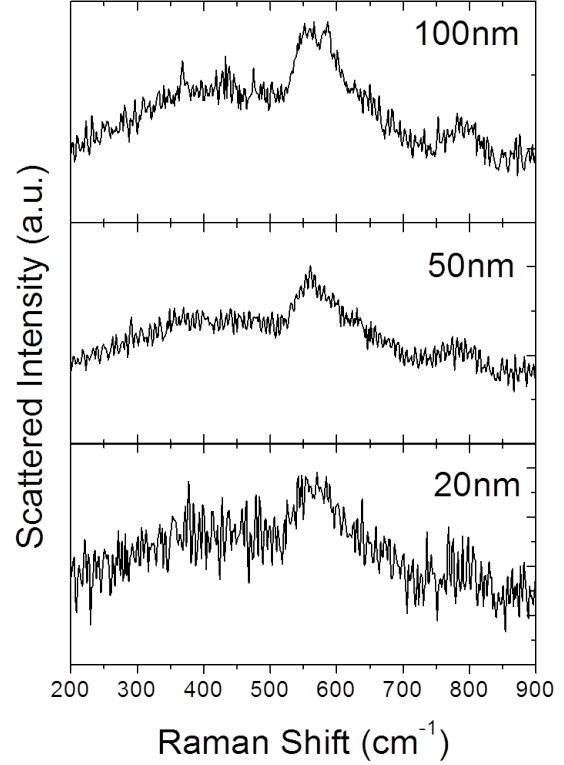


Figure 2: Spontaneous Raman Spectra of ZnO thin films.

Mode	ZnO Single Crystal (cm^{-1}) [Ben08]	ZnO Film (cm^{-1}) [Shi13]	ZnO Bulk (cm^{-1}) [Pin83]	ZnO nanostructured film (cm^{-1})
E_2^{low}	101			
E_2^{high}	444	435	434	425 - 450
A_1 (TO)	380	380	375	350 - 371
E_1 (TO)	413		405	
A_1 (LO)	579	577	578	574 - 577
E_1 (LO)	591			

Table 1: Experimental values of ZnO active modes found in the literature compared with the present job.

On one hand, we can observe the three Raman bands belonging to ZnO phonons (see table 1) in the three thin films: the first Raman band is related to the Raman band $A_1(\text{TO})$ at 380 cm^{-1} , the second one is related to the Raman band E_2^{high} at 435 cm^{-1} , and the third one is related to the Raman band $A_1(\text{LO})$ at 577 cm^{-1} . So, all these Raman bands found in the thin films are related to the characteristic vibration modes of the oxygen atom in the ZnO structure. Furthermore, we can add that the variation of the Raman signal of $A_1(\text{LO})$ band at 577

cm^{-1} in the three samples, which is a consequence of the presence of zones rich in zinc, therefore it decreases the presence of oxygen atoms in the nanocolumns by decreasing the area (intensity) of the band, which as we mentioned is linked to the oscillation of the oxygen atom. On the other hand, we have observed a Raman band that appears at approximately 780 cm^{-1} , which is not a characteristic vibration mode of ZnO (see Table 2), which is very far from the observed E_1 (TO) mode at 591 cm^{-1} in ZnO single crystals. Also, we have observed

increasing of values on displacement of the position ω , full width half maximum profile Γ , and Area of ZnO Raman bands from 100 to 20 nm. Moreover, Gouadac *et al* [Gou07] claim that two kinds of parameters will influence the spectra: a) parameters like atomic mass, bond strength or the system geometry (interatomic distance, atomic substitutions) will set the Raman bands positions, and b) parameters like ionic-covalency, band structure, electronic insertion will set intensity, on the basis of the vibration-induced charge variations occurring at the very bond scale. Additionally, Arguello *et al* [Arg69] mentioned that the Raman shift ω , as the width of the mode Γ , strongly depend on the zinc isotope and oxygen atom; in our case, thin films depend on the nature of the ZnO compound, which presents inherent structural defects, as we will comment in the next paragraph.

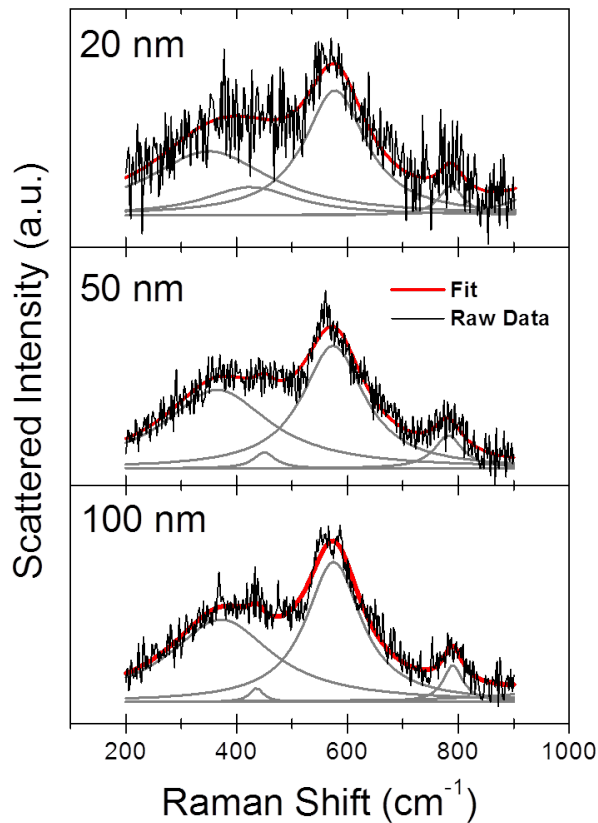


Figure 3: Fitted spontaneous Raman spectra with Lorentzian profiles.

Therefore, the fact that a pronounced widening is observed in some Raman band could indicate that the majority of intrinsic defects present in our ZnO nanostructured thin films are related better to zinc than oxygen atom, as mentioned in the previous paragraph. In

this sense, the changes observed in Raman band position are mainly related to defects and broken translation symmetry that affect the bond strength between Zn and O atoms in the unit cell, as specially observed in A_1 (TO) and E_2^{high} phonon modes, and in minor scale in A_1 (LO). Moreover, the difference detected among the width of the Raman bands (Γ) are linked to increasing of crystallinity of nanocolumns in the thin films. Additionally, the modification on Raman phonon intensities are connected to light variation in the ZnO band structure due to electronic density modification in the unit cell. On the one hand, the Raman band at 800 cm^{-1} can be, relates to the breaking of the vibration symmetry in the ZnO structure, that is, the existence of Zn-rich zones at nanometric scale within of nanocolumns matrix; or loss of translational symmetry in all the film as a consequence of the nanocolumnar microstructure. On the other hand, this band at 800 cm^{-1} may also be related to disorder in the thin film due to the low connectivity between the ZnO nanocolumns or low packing morphology, as is the case of thin porous films growth by sputtering process [Bar16] (see microimage in figure 3 in reference [Urb20]).

Parameter	Phonon mode	Film 1 20 nm	Film 2 50 nm	Film 3 100 nm
ω_1 (cm^{-1})	A_1 (TO)	350.0	364.9	371.9
Γ_1 (cm^{-1})	A_1	268.7	229.6	224.7
ω_2 (cm^{-1})	E_2^{high}	8505.01	8315.7	6715.1
Γ_2 (cm^{-1})	A_2	425.0	450.0	435.0
ω_3 (cm^{-1})	A_1 (LO)	206.5	46.7	30.0
Γ_3 (cm^{-1})	A_2	2880.7	347.7	150.0
ω_4 (cm^{-1})	A_1 (LO)	577.5	574.4	574.9
Γ_4 (cm^{-1})	A_3	135.7	136.4	121.5
ω_5 (cm^{-1})	A_3	8382.5	7722.1	6162.9
ω_6 (cm^{-1})	A_4	787.3	782.1	790.4
Γ_6 (cm^{-1})	A_4	52.7	61.3	42.7
χ^2		783.3	938.7	570.9
		0.69881	0.88546	0.91098

Table 2: Fitted values of ZnO phonons.

Continuing with the optical characterization of the ZnO thin films, we have exploited the configuration of Raman spectrometer in order to assess the photoluminescence of the samples. UV laser at 325 nm was used as exciting source of photoluminescence in the ZnO nanocolumns. Figure 4 displays the micro-photoluminescence spectra consists mainly of two intense emission bands. The first emission band placed in the ultraviolet region (centered around 380 nm) corresponds to the band near the emission edge which is attributed to the excitonic states [Bag97], the other emission band is found in the visible region (centered around 530 nm),

called green emission, which is due to structural defects, such as: oxygen vacancies, interstitial Zn atoms, and Zn vacancies [Kan04].

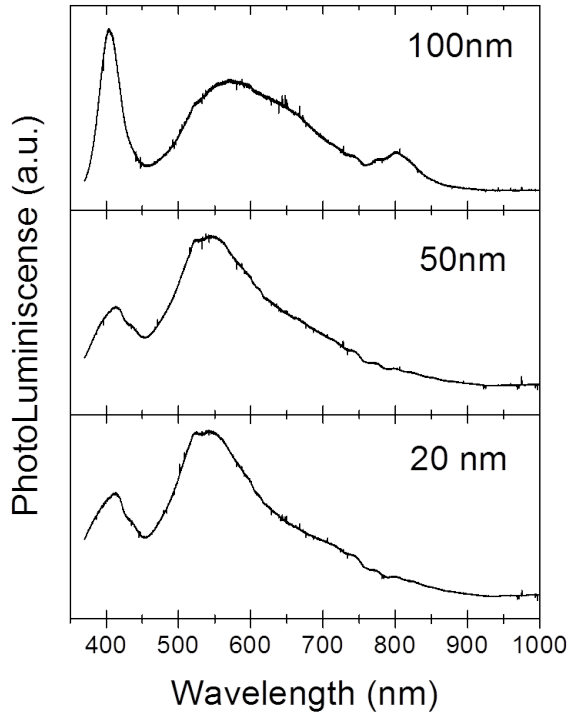


Figure 4: Photoluminescence spectra of ZnO thin films.

The emission spectra seen in figure 4 confirm that ZnO nanostructured thin films shown photoluminescent properties. The UV laser spot size $\sim 2.5 \mu\text{m}$ in diameter includes a large colony of ZnO nanocolumns (nanocolumns size in the order of 50 nm [Urb20]). Additionally, in figure 4, the photoluminescence signal in the 100 nm layer shows an improvement in the UV emission band as consequence of increasing of the volume interaction, but the green emission deteriorates, presenting a convolution of other signals in the near-infrared. Therefore, figure 5 presents the photoluminescence spectra adjusted with Lorentzian profiles and Table 3 shows the fitted parameters obtained, such as: band position λ (nm), band width Γ (nm), area A. The values of the figures of merit (χ^2) for the three thin films of 20, 50 and 100 nm were 0.99146, 0.99213, and 0.98372, respectively. According to the fitted values presented in Table 3, ZnO films of 20 nm and 50 nm show fit profiles with three emission bands, centered around 404 nm, 543 nm and 660 nm approximately; while ZnO films of 100 nm have emission bands centered around 790 nm and 811 nm, additional to the three emission bands mentioned before. As described in the first paragraph of this section, the photoluminescence spectra of ZnO consist mainly of two emission bands: one in UV and the other one in

visible, which corresponds to the ZnO emission bands found in literature. Moreover, the UV and green emission bands of the films shown a clear blue shift.

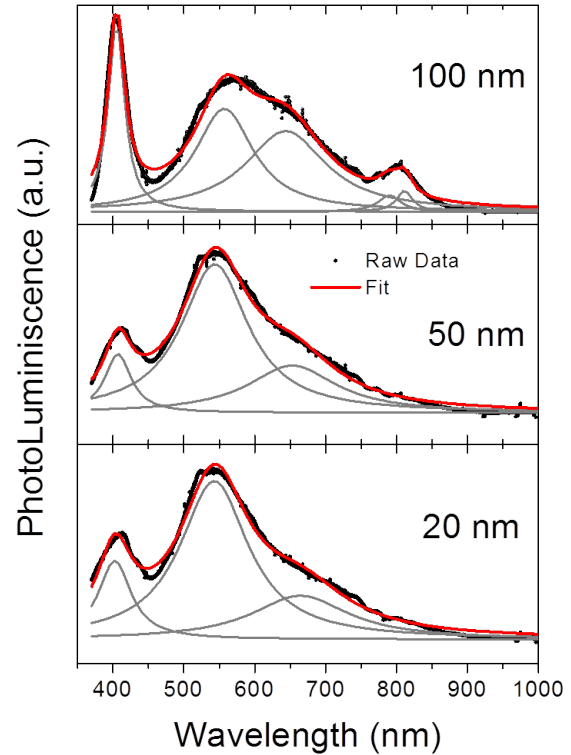


Figure 5: Fitted photoluminescence spectra with Lorentzian profiles.

At the light of the results, we can argue that the appearance of emission bands upper to 560 nm could be the result of localization of Zn-rich zones in the ZnO nanocolumns as Lopez *et al* [Lop11] claims, as a product of ZnO nanocolumnar growth by sputtering process in oxygen reactive atmosphere; that is, very small regions of Zn nanocrystals exist within of ZnO nanocolumns. This result obtained correlates very well with the Raman measurements of its Raman band around 780 cm^{-1} linked to disorder in the thin film due to low connectivity among ZnO nanocolumns or low packing morphology as consequence of porosity; as well as the results obtained from the X-ray diffraction [Urb20] about increasing of the texture in the nanocolumns through the increasing of (002) profile. Therefore is possible to argue that the ZnO nanocolumns grow in (002) direction, where colonies of Zn-rich zones were created at nanometric scale [Lop16], due to decreasing of oxygen atoms as consequence of the same growth process by sputtering, the power of the Zn magnetron and the nature of ZnO compound outside of stoichiometry.

Parameter	Film 1 20 nm	Film 2 50 nm	Film 3 100 nm
λ_1 (nm)	402.5	406.9	404.9
Γ_1 (nm)	56.0	44.9	27.4
A_1	566570.0	264744.6	158056.7
λ_2 (nm)	542.8	543.7	557.1
Γ_2 (nm)	117.2	114.1	99.9
A_2	2388890.0	1696860.0	312663.2
λ_3 (nm)	664.3	652.8	643.7
Γ_3 (nm)	165.7	152.1	138.0
A_3	931062.9	718901.4	338280.2
λ_4 (nm)			790.0
Γ_4 (nm)			37.7
A_4			18762.8
λ_5 (nm)			811.3
Γ_5 (nm)			27.0
A_5			17213.9
χ^2	0.99146	0.99213	0.98372

Table 3: Fitted values of ZnO emission bands.

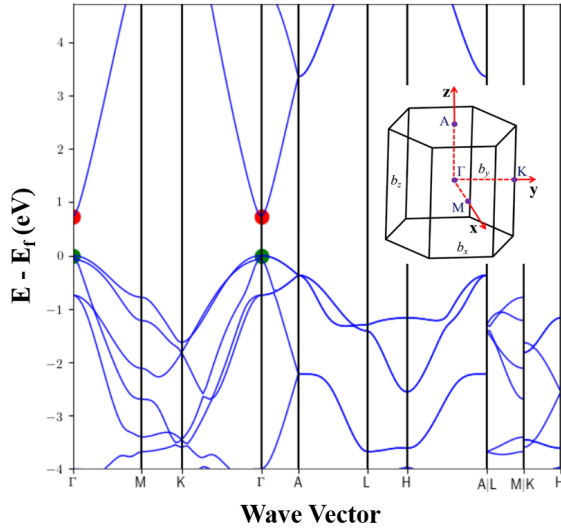
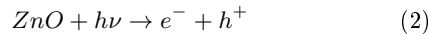


Figure 6: ZnO band structure (Adapted from reference [Jai13]).

The photoluminescence process in ZnO can be described by the following equation [Rom10]:



where $h\nu$ is the energy of photon incident, e^- and h^+ are electron and hole, the carrier charges involved in the creation of exciton. Figure 6 illustrates a picture of this

exciton (quasiparticle formed by an electron and a hole linked by Coulomb interaction) in the ZnO band structure denoted by one electron in the conduction band (circle color red) and one hole in the valence band (circle color green).

Conclusions

Using Raman spectroscopy we found bands belonging to ZnO, which were: band A_1 (TO) at 380 cm^{-1} , band E_2^{high} at 435 cm^{-1} and band A_1 (LO) at 577 cm^{-1} . The fitting with Lorentzian profiles of the Raman spectra enabled to obtain the values of the position of the band ω (cm^{-1}), width of the profile Γ (cm^{-1}) as well as the area A . Likewise, the band observed at 780 cm^{-1} was related to the Zn-rich zones, texturing of the nanocolumns as well as the poor connectivity between the nanocolumns, which then results in breaking-symmetry of vibration in ZnO structure.

The photoluminescence spectroscopy performed shows luminescence in all three thin films. A blue shift of all bands was observed. Two emission bands were obtained: UV (centered at 400 nm) and visible (centered at 550 nm). The fitting with Lorentzian profiles of the spectra allowed to obtain the values of the position of the band λ (nm), width of the profile Γ (nm) as well as area A . The 100 nm thin film has the best UV emission band but unwanted emission bands in the near-infrared. The appearance of the bands at 790 and 811 nm is related to the location of nanocrystals of Zn-rich colonies in the nanocolumn matrix, correlating them with the Raman phonon band at 780 cm^{-1} .

Acknowledgments

Authors deeply thanks to three agencies: British Council (UK), CONCYTEC FONDECYT (Peru) and Consejo Superior de Investigaciones Científicas (Spain) whom funded the research projects: Nanostructured magnetic thin films of functional oxide for developing of electronic devices based on spintronic; and Crecimiento de nanoestructuras columnares mediante la técnica de magnetron sputtering con aplicaciones tecnológicas; and Planar photonic structures for development of optofluidics sensors and harnessing of solar energy, respectively. JC Gonzalez thanks to Prof. Agustin R. Gonzalez-Elipse from Materials Science Institute of Seville – CSIC for allowed us to perform Raman and photoluminescence measurements with RH800 Horiba-Jobin-Yvon spectrometer.

References

- [Alv14] Alvarez, R., Lopez-Santos, C., Parra-Barranco, J., Rico, V., Barranco, A., Cotrino, J., Gonzalez-Elipe, A. R., Palmero, A. (2014) Nanocolumnar growth of thin films deposited at oblique angles: Beyond the tangent rule. *J. Vac. Sci. Technol. B* **32**, 041802 <https://doi.org/10.1116/1.4882877>
- [Arg69] Arguello, C., Rosseau, D., Porto, S. (1969) First-Order Raman Effect in Wurtzite-Type Crystals. *Phys. Rev.* **81**, 1351 <https://doi.org/10.1103/PhysRev.181.1351>
- [Bar16] Barranco, A., Borrás, A., Gonzalez-Elipe, A., Palmero, A. (2016) Perspectives on oblique angle deposition of thin films: From fundamentals to devices. *Progress in Materials Science* **76**, 59 <http://dx.doi.org/10.1016/j.pmatsci.2015.06.003>
- [Bag97] Bagnall, D., Chen, Y., Zhu, Z., Yao, T. (1970) Optically pumped lasing of ZnO at room temperature. *Appl. Phys. Lett.* **70**, 2230 <https://doi.org/10.1063/1.118824>
- [Ben08] Ben Yahia, S., Znaidi, L., Kanaev, A., Petitet, J. (2008) Raman study of oriented ZnO thin films deposited by sol-gel method. *Spectrochimica Acta Part A* **71**, 1234 <https://doi.org/10.1016/j.saa.2008.03.032>
- [Bha05] Bhat, S., Deepak, F. (2005) Tuning the band gap of ZnO by substitution with Mn^{2+} , Co^{2+} and Ni^{2+} . *Solid State Communications* **135**, 345 <https://doi.org/10.1016/j.ssc.2005.05.051>
- [Cul56] Cullity, B. (1956). *Elements of X-ray Diffraction*. USA: Addison Wesley Publishing Company Inc..
- [Gou07] Gouadec, G., Colomban, P. (2007) Raman spectroscopy of nanomaterials: how Spectra relate to disorder, particle size and mechanical properties. progress in crystal growth and characterization of materials. *Prog. Cryst. Growth Charact. Mater.* **53** (1), 1 <https://doi.org/10.1016/j.pcrystgrow.2007.01.001>
- [Ish06] Ishikawa Y, Shimizu Y, Sasaki T and Koshizaki N (2006) Preparation of zinc oxide nanorods using pulsed laser ablation in water media at high temperature. *J. Coll. Int. Sc.* **300**, 612 <https://doi.org/10.1016/j.jcis.2006.04.005>
- [Jai13] Jain, A., Ong, S., Hautier, G., Chen, W., Davidson Richards, W., Dacek, S., Cholia, S., Gunter, D., Skinner, D., Ceder, G., Persson, K. (2013) Commentary: The Materials Project: A materials genome approach to accelerating materials innovation. *APL Mater.* **1**, 011002 <https://doi.org/10.1063/1.4812323>
- [Kan04] Kang, H., Kang, J., Kim, J., Lee, S. (2004) Annealing effect on the property of ultraviolet and green emissions of ZnO thin films. *J. Appl. Phys* **95**, 1246 <https://doi.org/10.1063/1.1633343>
- [Ko003] Ko, S., Kim, Y., Lee, S., Choi, S., Kim, S. (2003) Micro machined piezoelectric membrane acoustic device. *Sensors and Actuators* **103**, 130 [https://doi.org/10.1016/S0924-4247\(02\)00310-2](https://doi.org/10.1016/S0924-4247(02)00310-2)
- [Lop11] Lopez, R., Díaz, T., Rosendo, E., García, G., Coyopol, A., Suarez, H. (2011) Propiedades fotoluminiscentes de películas de ZnO:A-SiOx obtenidas por la técnica CVD asistido por filamento caliente. *Rev. Lat. Metalur. y Mater.* **31**, 59 http://ve.scielo.org/scielo.php?script=sci_arttext&pid=S0255-69522011000100009
- [Lop16] Lopez-Santos, C., Alvarez, R., Garcia-Valenzuela, A., Rico, V., Loeffler, M., Gonzalez-Elipe, A. R., Palmero, A. (2016) Nanocolumnar association and domain formation in porous thin films grown by evaporation at oblique angles. *Nanotechnology* **27**, 395702 <https://doi.org/10.1088/0957-4484/27/39/395702>
- [Pan01] Pan, Z., Dai, Z., Wang, Z. (2001) Nanobelts of semiconducting oxides, *Science* **291**, 1947 <https://doi.org/10.1126/science.1058120>
- [Pin83] Pinczuk, A., Burstern, E. (1983) Fundamentals of Inelastic Light Scattering in Semiconductors and Insulators. Chapter 2, page 3 in *Light Scattering in Solids I: Introductory Concepts*. Manuel Cardona Eds. Germany, Springer-Verlag Berlin Heidelberg
- [Pol08] Polyanskiy, N. (2008) Refractive index database web: <https://refractiveindex.info>
- [Rom10] Romero-Gómez, P., Toudert, J., Sánchez-Valencia, J., Borrás, A., Barranco, A., Gonzalez-Elipe, A. (2010) Tunable nanostructure and photoluminescence of columnar ZnO films grown by plasma deposition. *J. Phys. Chem. C* **114** (49), 20932 <https://doi.org/10.1021/jp103902u>
- [Shi13] Shinde, K., Dhoble, K., Swart, S., Park, H. (2013) Phosphate Phosphors for Solid-State Lighting. Chapter 2, page 41 in *Springer Series in Materials Science 174*. Germany, Ed. Springer-Verlag Berlin Heidelberg.

- [Urb20] Urbina Yarupetan, M., Gonzalez, J.C. (2020) Microstructural study and characterization of ZnO thin films. *Rev. Inv. Fis.* **23** (2) https://fisica.unmsm.edu.pe/rif/previo_files/2020-2/04urbina.pdf
- [Veg14] Vega-Poot, A., Macías-Montero, M., Idígoras, J., Borrás, A., Barranco, A., González-Elipe, A., Lizama-Tzec, F., Oskam, G., Anta, J. (2014) Mechanisms of Electron Transport and Recombination in ZnO Nanostructures for Dye-Sensitized Solar Cells. *Chem. Phys. Chem.* **15**, 1088 <https://doi.org/10.1002/cphc.201301068>
- [Wan04] Wang, Z. (2004) Nanostructures of zinc oxide. *Materials today* **7**, 26 [https://doi.org/10.1016/S1369-7021\(04\)00286-X](https://doi.org/10.1016/S1369-7021(04)00286-X)
- [Wan08] Wang, Z. (2008) Oxide nanobelts and nanowires -growth, properties and applications. *J. Nanosci.Nanotechnol.***8**, 27 - 55 <https://doi.org/10.1166/jnn.2008.N08>
- [Yua17] Yuan, X., Mayanovic, R. (2017) An empirical study on Raman peak fitting and its application to Raman quantitative research. *Appl. Spectrosc.* **71**, 2325 <https://doi.org/10.1177/0003702817721527>
- [Zho06] Zhou, J., Xu, N., Wang, Z. (2006) Dissolving behavior and stability of ZnO wires in biofluids: A study on biodegradability and biocompatibility of ZnO nanostructures. *Adv. Materials* **18**, 2432 <https://doi.org/10.1002/adma.200600200>